

Engineering Notes

Dye Visualization of the Flow Structure over a Yawed Nonslender Delta Wing

C. Canpolat,* S. Yayla,* B. Sahin,† and H. Akilli‡
Cukurova University, 01330 Balcali, Turkey

DOI: 10.2514/1.45274

I. Introduction

STUDIES of aerodynamic structures and behaviors of the non-slender delta wings are invariably essential to develop a method to control the development of the vortex breakdown as well as the development of vortices. Unsteady aerodynamics of nonslender delta wings, consisting of shear layer instabilities, the structure of vortices, the occurrence of breakdown, and fluid/structure interactions were extensively reviewed by Gursul et al. [1]. They emphasized the sensitivity of the vortical flow structures varying the angle of attack α of the delta wing. Yavuz et al. [2] studied the vortical flow structure on a plane immediately adjacent to the surface of nonslender delta wing, $\Lambda = 38.7$ deg. Yaniktepe and Rockwell [3] performed experimental investigations on the flow structures at trailing-edge regions of diamond- and lambda-type wings. In both wings, vortical flow structures in the crossflow planes of trailing edge vary rapidly with the angles of attack α . Sohn et al. [4] visually investigated the development and interaction of vortices in crossflow planes at various locations on the delta wing with leading edge extension (LEX) using micro water droplets and a laser beam sheet. The range of angle of attack α was taken as $12 \leq \alpha \leq 24$ deg at yaw angles θ of 0, -5 , and -10 deg. It was indicated that, by introducing yaw angle θ , the coiling, merging, and diffusion of the wing and LEX vortices increased on the windward side, whereas they became delayed significantly on the leeward side. Their study confirmed that the yaw angle θ had a profound effect on the vortex structures. Taylor and Gursul [5] visualized leading-edge vortices of a $\Lambda = 50$ deg sweep angle, having angles of attack as low as $\alpha = 2.5$ deg. Gursul et al. [6] report that combat air vehicles (UCAVs) and micro air vehicles have particularly dominant vortical flows having low sweep angles (25 – 55 deg), and future UCAVs are expected to be highly maneuverable and highly flexible. Yaniktepe and Rockwell [7] aimed at investigating the unresolved concepts, which included averaged structure of shear layer from the leading edge of the wing, unsteady features of separated layer adjacent to the surface of the wing, and control of flow structure by leading-edge perturbations. Elkhoury and Rockwell [8] have investigated to provide various measurements of the visualized dye patterns, including the degree of interaction of vortices, the onset of vortex breakdown, and effective sweep angle of the wing root vortex, as a function of both Reynolds number and angle of attack α . Elkhoury et al. [9] had investigated the

Reynolds number dependence of the near-surface flow structure and topology on a representative UCAV planform.

The present investigation focuses on the formation and development of leading-edge vortices, vortex breakdown, and three-dimensional separation and stall of the complex and disorganized flow structure over the delta wing. The leading-edge sweep angle was $\Lambda = 40$ deg. The angle of attack was varied within the range of $7 \leq \alpha \leq 17$ deg and the yaw angle θ was varied within the range of $0 \leq \theta \leq 15$ deg.

II. Experimental System

Experiments were conducted on a large-scale circulating free-surface water channel. The internal dimensions of the water channel were $8000 \times 1000 \times 750$ mm, which was made from a 15-mm-thick transparent Plexiglas sheet with upstream and downstream fiberglass reservoirs. Before reaching the test chamber, the water was pumped into a settling chamber and passed through a honeycomb section and a 2:1 channel contraction. These reservoirs and honeycomb screen arrangements were used to maintain the turbulence intensity below 0.1%. The wing was initially maintained in a horizontal position by a slender support strut that extended vertically from the midchord of the wing. A fluorescent dye, which shined under the laser sheet, was used to create color change in the water to visualize flow characteristics over the delta wing during the dye experiments. Dye was injected in the near field of the delta wing trailing edge by plastic pipe, and dye was passed through a narrow and close channel in the delta wing to its apex. The video camera (Sony HD-SR1) was used to capture the instantaneous video images of the vortex flow structures. The delta wing had a chord length of $C = 140$ mm with a sweep angle of $\Lambda = 40$ deg. The schematic of the experimental arrangement, including laser sheet orientations and corresponding parameters, is presented in Fig. 1. The depth of the water in the test section was adjusted to 530 mm for the present experiments. The Reynolds number based on the delta wing chord was kept constant for all experiments as $Re_c = 10,000$, which corresponded to the freestream velocity of 72 mm/s for all experiments. The flow characteristics over the delta wing in the plan-view plane was presented for angles of attack such as $\alpha = 7, 10, 13$, and 17 deg, and yaw angles such as $\theta = 0, 6, 8$, and 15 deg. Dye visualization experiments in the crossflow plane were performed at locations of $X/C = 0.6, 0.8$, and 1. On the other hand, for the plan-view measuring planes, the laser sheet was located along the central axes of leading-edge vortices.

III. Results and Discussion

The behavior of flow structure of the delta wing in the side-view plane is presented for different angles of attack in Fig. 2. As seen in the first image, a coherent leading-edge vortex is formed very close to the delta wing surface, having an angle of attack of $\alpha = 7$ deg. As seen in the work of Ozgoren et al. [10] and Akilli et al. [11], the leading-edge vortex takes place further away from the surface of the slender delta wing compared to the present delta wing. In addition, the primary vortex structures are more coherent in the case of slender delta wings (Sahin et al. [12]). The location of vortex breakdown moves toward the apex of the delta wing rapidly when the angle of attack α increases slightly. For example, the vortex breakdown occurs at the delta wing apex at an angle of attack of $\alpha = 13$ deg. In the present dye visualization, it was demonstrated that the vortex breakdown location shows significant fluctuations in the streamwise direction, as also stated by Ol and Gharib [13] and Taylor et al. [14]. A large-scale separation/stall is developed over the entire surface of the wing under a high angle of attack α presented in the third and fourth images of Fig. 2, as also stated by

Received 4 May 2009; revision received 12 July 2009; accepted for publication 14 July 2009. Copyright © 2009 by the American Institute of Aeronautics and Astronautics, Inc. All rights reserved. Copies of this paper may be made for personal or internal use, on condition that the copier pay the \$10.00 per-copy fee to the Copyright Clearance Center, Inc., 222 Rosewood Drive, Danvers, MA 01923; include the code 0021-8669/09 and \$10.00 in correspondence with the CCC.

*Research Assistant, Department of Mechanical Engineering, Faculty of Engineering and Architecture, Adana.

†Professor, Department of Mechanical Engineering, Faculty of Engineering and Architecture, Adana.

‡Associate Professor, Department of Mechanical Engineering, Faculty of Engineering and Architecture, Adana.

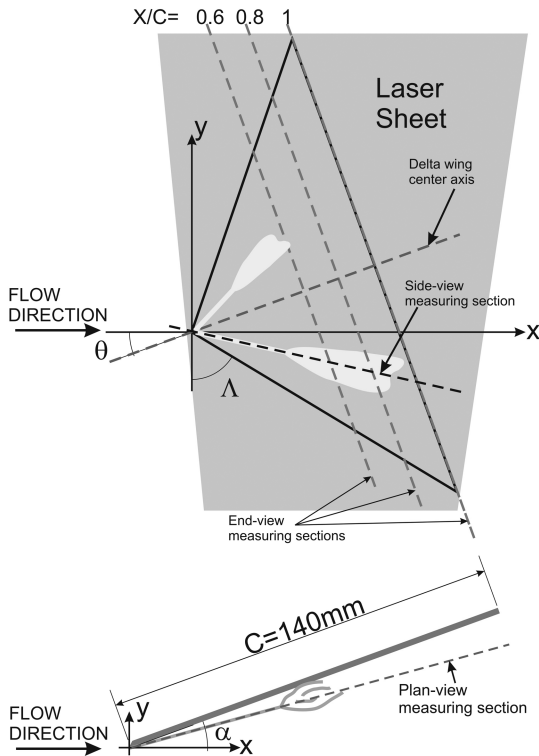


Fig. 1 Schematic of experimental arrangement including laser sheet orientations and corresponding parameters.

Yaniktepe and Rockwell [7]. Examining all images indicates that high-scale Kelvin–Helmholtz vortex structures occur at the bottom of the unsteady flow region, especially for the angles of attack of $\alpha = 13$ and 17 deg. There is a strong interaction between vortical flow and wing surface. The angle between the delta wing and central axis of the coherent leading-edge vortex slightly increases when the angle of attack increases from $\alpha = 7$ to 13 deg. The separated flow occupies the surface of the delta wing completely beyond $\alpha > 13$ deg.

Images of the coherent leading-edge vortex and vortex breakdown over the delta wing surface in the plan-view plane for the angle of attack $\alpha = 10$ deg and yaw angle $\theta = 10$ deg are presented in Fig. 3. Initially, the leading-edge vortex is arced starting from the apex of the wing due to the effect of yaw angle θ , and later this curved leading-edge vortex turns into an elongated shape and continues to

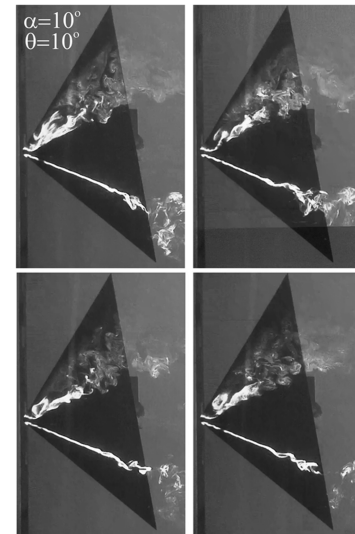


Fig. 3 Formation and development of leading-edge vortex and vortex breakdown observed in plan-view plane.

rotate around a straight line as a leading-edge vortex. Next to the curved part of the leading-edge vortex, a small swirling-type (focus) vortex takes place, rotating about its axis, which is perpendicular to the measuring plane. The domain of this focus enlarges its size time to time on a quasi-periodic basis. When this focus gets its largest shape, the leading-edge vortex disintegrates causing vortex breakdown in the upper stage close to the apex.

The vortex on the leeward side of the delta wing is maintained by the leading-edge vortices as well as being supported by the flow coming from the top side of the delta wing. In this way, the separated shear layer is kept steady and the occurrence of the vortex breakdown is delayed. On the contrary, the vortex on the windward side of the delta wing cannot be supported sufficiently by the flow coming from the top side of the delta wing, because the yaw angle has an effect on decreasing the sweep angle on the windward side, whereas the yaw angle has an effect on increasing the sweep angle on the leeward side. Therefore, vortex breakdown occurs on the windward side at an early stage compared to the case of zero yaw angle.

The results of dye visualization experiments at angles of attack $\alpha = 7, 10, 13$, and 17 deg and having yaw angles of $\theta = 0, 4, 8, 10$, and 15 deg are shown in Fig. 4. In the first row of Fig. 4, having $\alpha = 7$ and 10 deg, coherent leading-edge vortices emanating from the delta wing leading edge are clearly identifiable, and it is clear that vortex breakdowns occur after a certain distance from the delta wing apex at a wandering locations. As seen in the first row of Fig. 4, there is a symmetrical flow structure over the delta wing on both sides of the central axis in the case of zero yaw angle θ in macroscale. In addition, the leading-edge vortex breakdown locations move in the upstream direction by a large L_{vb}/C fraction over a small range of angle of attack such as $10 < \alpha < 13$ deg. Having a yaw angle less than $\theta = 4$ deg at an angle of attack of $\alpha = 7$ deg, the flow structure over the surface of the delta wing is nearly symmetric in macroscale. When the yaw angle θ increases beyond $\theta = 4$ deg, the symmetrical flow structure on both sides of the chord axis of the delta wing begins to deteriorate. For instance, the vortex breakdown location on the leeward side of the delta wing begins to delay compared to the windward side of the delta wing. The secondary vortex next to the leading-edge vortex appears at yaw angles of $\theta = 8, 10$, and 15 deg for the angle of attack $\alpha = 7$ deg. Vortex breakdown occurs downstream of the trailing edge on the leeward side of the wing at $\alpha = 7$ deg and $\theta = 15$ deg. It can be concluded that the yaw angle becomes effective when its value is higher than $\theta = 6$ deg. The windward side leading-edge vortex axis shifts its location toward the central chord axis and the vortex breakdown occurs at a location further upstream in the case of higher yaw angle θ . Although the angle of attack is set to $\alpha = 10$ deg in the second images of Fig. 4, both leading-edge vortices exist for all cases of yaw angle θ on the leeward side. When the yaw angle increases from $\theta = 10$ to

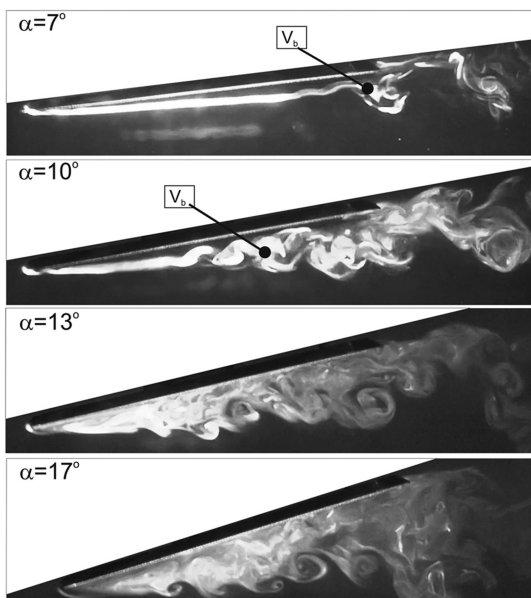


Fig. 2 Dye visualization of flow in side-view plane over the delta wing.

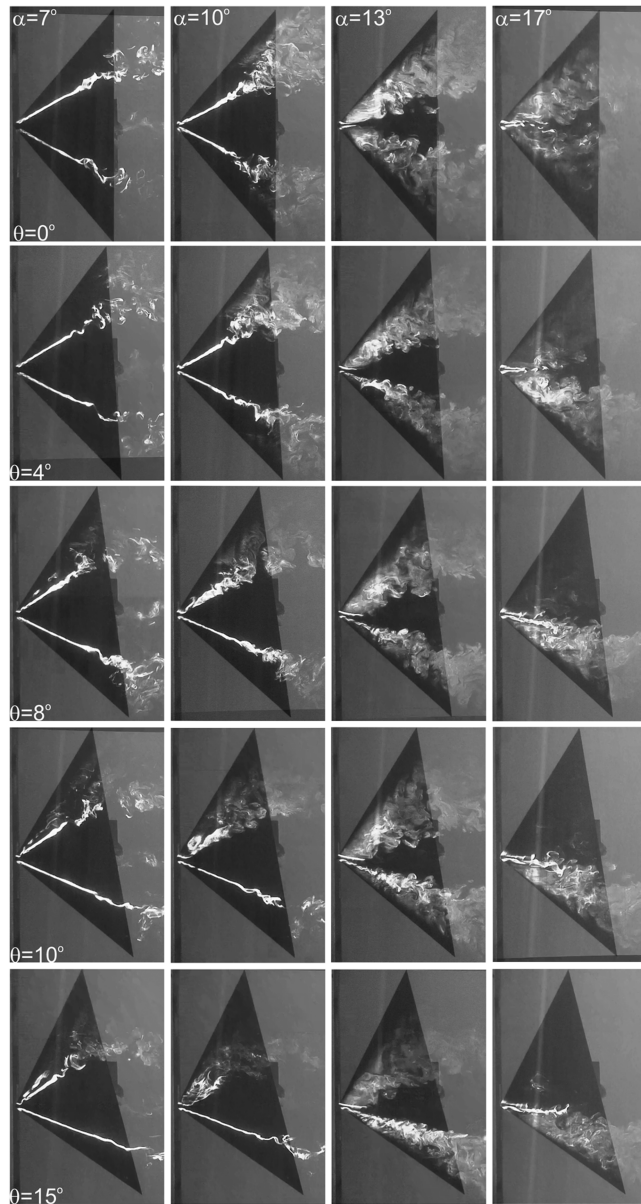


Fig. 4 Formation and development of a leading-edge vortex, the vortex breakdown, and the separated flow region as a function of angle of attack α and yaw angle θ .

$\theta = 15$ deg, as seen in the second column of Fig. 4, the area of the swirling-type vortex increases and the vortex breakdown location moves further downstream on the leeward side of the delta wing. On the upper region of the midchord axis of the delta wing, a separated flow takes place at $\theta \geq 10$ deg along the windward side of side wing. Adjusting the angle of attack to a value of $\alpha = 13$ deg and yaw angle to a value of $\theta = 0$ deg, a swirling-type flow is developed in a close region of the apex of the delta wing. But having an angle of attack of $\alpha = 13$ deg and a yaw angle of $\theta = 4$ deg, the swirling-type vortex only exists on the windward side of the central (midchord) axis of the delta wing, whereas, on leeward side, this swirling-type vortex turns into a coherent leading-edge vortex. A similar vortical flow structure takes place even increasing the yaw angle up to $\theta = 15$ deg. A certain portion of the wing is not covered by dye along the central axis of the wing due to the streamwise velocity which swept away the dye continuously due to increasing the sweep angle on the windward side. On the other hand, increasing the angle of attack furthermore to a value of $\alpha = 17$ deg, no more leading-edge vortex is developed over the delta wing for all cases of yaw angle. Separated flow occupies the whole surface of the delta wing. It is also quite difficult to see the swirl-type flow motion close to the apex of the delta wing beyond $\theta = 10$ deg.

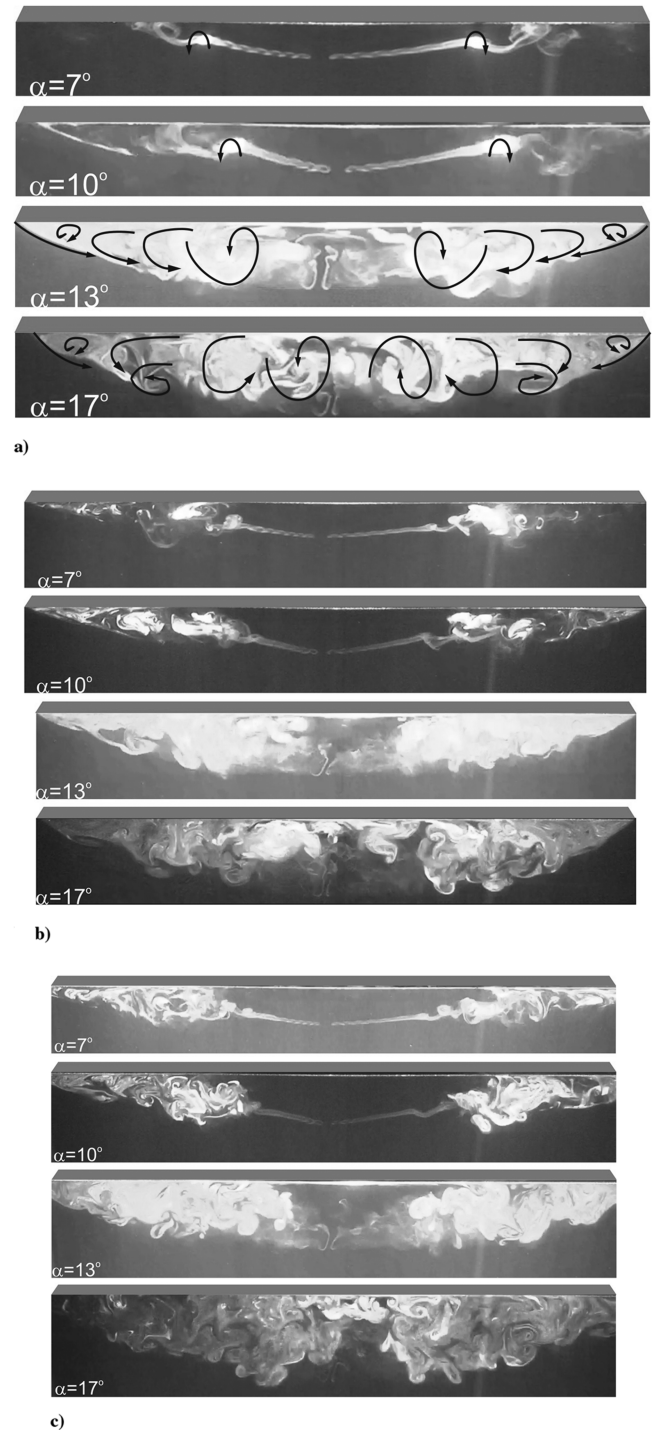


Fig. 5 Formation and development of a vortex structure in end-view plane in the case of zero yaw angle at a) $X/C = 0.6$, b) $X/C = 0.8$, and c) $X/C = 1$.

Dye observation was conducted in three different end-view planes, such as $X/C = 0.6, 0.8$, and 1 , as shown in Fig. 5, to study vortical flow structure at a crossflow plane further downstream of the vortex breakdown. As soon as vortex breakdown occurs, a coherent leading-edge vortex core disintegrates into small-scale vortices. The main spanwise rotating vortices occur in the inner side of the leading edge close to the central axis of the delta wing. Small-size vortices are also developed next to the main rotating vortices. These secondary vortices get smaller in size when they move closer to the side edges of the delta wing. The outer line of the separated flow region gradually moves away from the surface of the delta wing as the end-view cross section is moved further downstream in the freestream flow direction. Between the surface of the delta wing and vortical flow structure, there is a strong interaction. The level of this interaction gets lower at

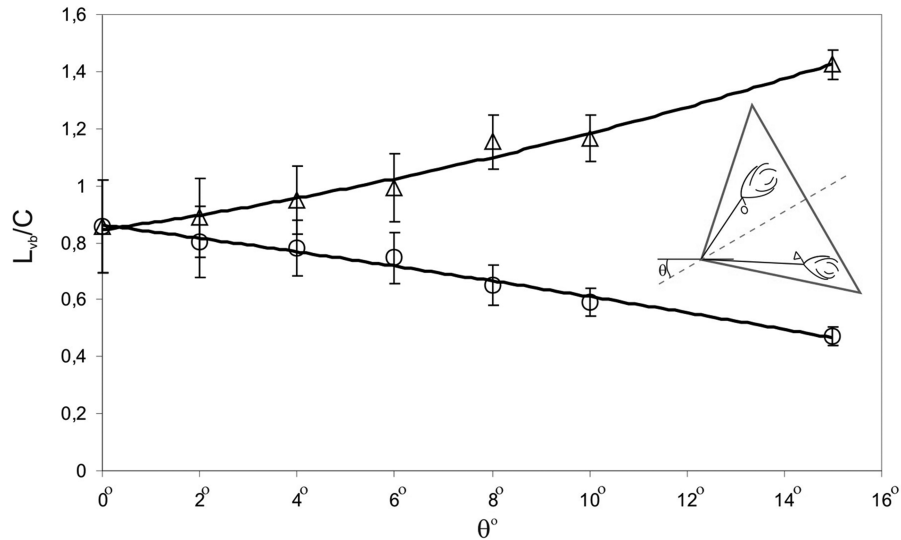


Fig. 6 Influence of the yaw angle θ on the vortex breakdown location from the delta wing apex, $\alpha = 7$ deg.

$X/C = 1$ compared to $X/C = 0.6$. The nonsteady flow structures caused by both leading-edge vortices have more or less the same vortical flow structure.

The influence of the yaw angle θ on the vortex breakdown location from the delta wing apex at angle of attack $\alpha = 7$ deg is presented in Fig. 6. The length of the vortex breakdown location from the delta wing apex L_{vb} was made dimensionless by dividing the delta wing chord length C . As mentioned before, when the yaw angle θ increases, the symmetrical flow structure on both sides of the chord axis of the delta wing deteriorates. The vortex breakdown location on the leeward side of the delta wing is delayed compared to the windward side of the delta wing. So, the differences between maximum and minimum lengths of vortex breakdown locations do not exceed $\pm 15\%$ of the chord length.

IV. Conclusions

Examining all dye visualization experiments, there is a symmetrical flow structure on the delta wing in the case of zero yaw angle θ . Also, there was a coherent pair of leading-edge vortices starting from the apex of the delta wing. The structure of these coherent leading-edge vortices decomposes developing vortex breakdown further downstream in the freestream flow direction. Examining all images in the side-view plane, it can be seen that a high-scale Kelvin-Helmholtz vortex structure occurs at the bottom of the unstable flow region, especially for the angles of attack of $\alpha = 13$ and 17 deg. When the delta wing is under the effect of a yaw angle θ , the symmetrical flow structure deteriorates and a vortex breakdown occurs earlier on the windward side of the delta wing as compared with the leeward side. The main rotating vortices in crossflow planes occur in the inner side close to the central axis of the delta wing. Small-size vortices are also evident next to the main rotating vortices.

Acknowledgment

The authors acknowledge the financial support of the Scientific and Technological Research Council of Turkey for funding under project no. 105M225.

References

- [1] Gursul, I., Gordnier, R., and Visbal, M., "Unsteady Aerodynamics of Nonslender Delta Wings," *Progress in Aerospace Sciences*, Vol. 41, No. 7, 2005, pp. 515–557.
doi:10.1016/j.paerosci.2005.09.002
- [2] Yavuz, M., Elkhoury, M., and Rockwell, D., "Near-Surface Topology and Flow Structure on a Delta Wing," *AIAA Journal*, Vol. 42, No. 2, 2004, pp. 332–340.
doi:10.2514/1.3499
- [3] Yaniktepe, B., and Rockwell, D., "Flow Structure on Diamond and Lambda Planforms: Trailing-Edge Region," *AIAA Journal*, Vol. 43, No. 7, 2005, pp. 1490–1500.
doi:10.2514/1.7618
- [4] Sohn, M. H., Lee, K. Y., and Chang, J. W., "Vortex Flow Visualization of a Yawed Delta Wing with Leading-Edge Extension," *Journal of Aircraft*, Vol. 41, No. 2, 2004, pp. 231–237.
doi:10.2514/1.9281
- [5] Taylor, G. S., and Gursul, I., "Buffeting Flows over a Low-Sweep Delta Wing," *AIAA Journal*, Vol. 42, No. 9, 2004, pp. 1737–1745.
doi:10.2514/1.5391
- [6] Gursul, I., Taylor, G., and Wooding, C. L., "Vortex Flows over Fixed-Wing Micro Air Vehicle," AIAA Paper 2002-0698, 2002.
- [7] Yaniktepe, B., and Rockwell, D., "Flow Structure on a Delta Wing of Low Sweep Angle," *AIAA Journal*, Vol. 42, No. 3, 2004, pp. 513–523.
doi:10.2514/1.1207
- [8] Elkhoury, M., and Rockwell, D., "Visualized Vortices on Unmanned Combat Air Vehicles Planform: Effect of Reynolds Number," *Journal of Aircraft*, Vol. 41, No. 5, 2004, pp. 1244–1246.
doi:10.2514/1.6290
- [9] Elkhoury, M., Yavuz, M. M., and Rockwell, D., "Near-Surface Topology of a Unmanned Combat Air Vehicles Planform: Reynolds Number Dependence," *Journal of Aircraft*, Vol. 42, No. 5, 2005, pp. 1318–1330.
doi:10.2514/1.9777
- [10] Ozgoren, M., Sahin, B., and Rockwell, D., "Structure of Leading-Edge Vortices on a Delta Wing at High Angle of Attack," *AIAA Journal*, Vol. 40, No. 2, 2002, pp. 285–292.
doi:10.2514/2.1644
- [11] Akilli, H., Sahin, B., and Rockwell, D., "Vortex Breakdown on a Delta Wing Controlled by a Coaxial Wire," *Physics of Fluids*, Vol. 15, No. 1, 2003, pp. 123–133.
doi:10.1063/1.1519261
- [12] Sahin, B., Akilli, H., Lin, J. C., and Rockwell, D., "Vortex Breakdown-Edge Intersection: Consequence of Edge Oscillations," *AIAA Journal*, Vol. 39, No. 5, 2001, pp. 865–876.
doi:10.2514/2.1390
- [13] Ol, M. V., and Gharib, M., "Leading-Edge Vortex Structure of Nonslender Delta Wings at Low Reynolds Number," *AIAA Journal*, Vol. 41, No. 1, 2003, pp. 16–26.
doi:10.2514/2.1930
- [14] Taylor, G. S., Schnorbus, T., and Gursul, I., "An Investigation of Vortex Flows over Low Sweep Delta Wings," AIAA Paper 2003-4021, 2003.